Korean J. Chem. Eng., 40(6), 1380-1388 (2023)
DOI: 10.1007/s11814-022-1326-6

pISSN: 0256-1115
eISSN: 1975-7220

Pyrolysis kinetics and thermodynamics of discarded Bakelite

Pabitra Mohan Mahapatra*, Achyut Kumar Panda*,†, Sahin Ahmed, and Sachin Kumar*****

*Department of Chemistry, Veer Surendra Sai University of Technology, Burla, Odisha, India, PIN 768018
**Department of Civil Engg., Veer Surendra Sai University of Technology, Burla, Odisha, India, PIN 768018
***Department of Energy Engineering, CoE-GEET, Central University of Jharkhand Brambe, Ranchi, India-835205
(*Received 20 July 2022 • Revised 4 October 2022 • Accepted 26 October 2022*)

Abstract−The thermal degradation kinetics of discarded Bakelite was studied by using different model fitting, model-free methods (Kissinger-Akahira-Sunose (KAS), Flynn-Wall-Ozawa (FWO), Friedman (FRM), Starink (STR), Li and Tang (LTA), Vyazovkin (VYZ), Avrami (AVM)) and Master plot (MP), for computing the kinetics triplets (A, Ea, and n) and also predict a suitable mechanism. The thermal degradation experiment of the sample was carried out from ambient to 1,000 °C at five different heating rates 5, 10, 20, 30, and 50 °C/min. under inert gas N_2 atmosphere. The thermal degradation of discarded Bakelite shows an order-based F_5 - model mechanism with the activation energy (Ea) of 213 KJ/mol, and the accuracy of the Ea was also proved by KAS, FWO, and VYZ iso-conversional method. The ordered-based model for the reaction mechanism was also explained by the master plot (MP). Based on the results of the non-linear method (VYZ), the mean error percentage of Ea, which is tested for various linear ways, was found to increase in the following order: FWO<KAS<STR<FRM<LTA and ranged from 0.115% to 23.492% for the degradation of discarded Bakelite. The change in free energy (ΔG), change in enthalpy (ΔH), and change in entropy (ΔS) are 560.743 KJ/mol, 100.835 KJ/mol, and -820.989×10^{-3} JK^{-1} mol^{-1}, respectively. The complete kinetic and thermodynamics analysis of the thermal degradation would help to design a process for the conversion of these wastes to high-valued carbonaceous products.

Keywords: Discarded Bakelite, Thermal Degradation, Kinetics, Model-free and Model Fitting Methods

INTRODUCTION

Bakelite or phenol-formaldehyde (PF) is a thermosetting resin that is utilized for cookware, jewelry, pipe stems, children's toys, guns, and electrical items like switches, boards, sockets, and wire insulation [1]. Bakelite was consumed in excess of 4 million tons globally in 2016 and the consumption rate grew year after year [2]. The size of the world market for phenolic resins was estimated at USD 11.74 billion in 2019 and it is expected to increase at a compound annual growth rate (CAGR) of 5.4% between 2020 and 2025 [3]. These thermosetting plastics are going to landfills and cause pollution. The noxious effect of Bakelite is due to the existence of free molecules like phenol, methyl alcohols, and ethyl alcohols and thus cause water pollution. Therefore, it is imperative to avoid the free disposal of Bakelite to prevent water contamination [4]. Thermosetting plastics are molded into the required shapes upon heating, but once they are cured these polymers are permanently settled and cannot be softened; thus they cannot be recycled or reused extensively [1]. To recycle or reuse Bakelite, it is necessary to invent useful approaches and technical beneficial methods.

There have been few studies on how to use and recycle discarded Bakelite. Toshihide et al. synthesized carbonized materials by combining phenol-formaldehyde (PF) resins with organic compounds like ethylene glycol (EG), and polyethylene glycol (PEG). The pore structure of carbonized phenol formaldehyde (CPF) depends upon the carbonization temperature, organic additive species, and additive ratio. The organic substance that was introduced had different molecular lengths, which led to variations in the pore sizes of the CPF. By adding short-chain compounds like EG, the pore size of the carbonized PFs gradually decreased as the carbonization temperature increased, whereas the pore size of the CPFs increased as the carbonization temperature increased by adding long-chain compounds like PEG with a molecular weight of 20,000 (PEG20K). The pore size of the carbonized PF is not changed largely by the additive ratio of EG. But compared to the carbonized PF without any additives, the average pore size variation is more pronounced. As opposed to that, the carbonized PFs possesses mesopores and larger pore diameters due to the high additive ratio of PEG20K [5]. Takuji et al. synthesized monodisperse carbon cryogel microspheres by utilizing a Shirasu porous glass membrane to emulsify a PF solution, followed by freeze-drying and carbonization in an inert environment [6]. Fitzer et al. produced glass-like carbon by pyrolyzing polyfurfuryl alcohol and phenolic resin. In each range of temperature, pyrolysis products are obtained in which no pores are detected by light and electron microscopy [7]. To produce phenolic-rich oil and char, PF resin is pyrolyzed using $Ca(OH)_2$ as a catalyst. According to Lijiang et al. after pyrolysis, the solid residue is heated to 800 °C to generate CaO/char material, which is employed as a catalyst to pyrolyze soybean oil for high-quality biofuel production. It is also shown that $Ca(OH)_2$ influences pyrol-

†To whom correspondence should be addressed.
E-mail: achyut.panda@gmail.com

ysis behavior and encourages PF resin to generate more monophenols during the pyrolysis process [2]. Through the self-assembly of PF and block copolymers under specially created aqueous basic or acidic conditions, Mingjiang et al. produced the ordered mesoporous carbon. At 313 K, the production of hydroxymethyl phenols is facilitated by the weakly basic condition. The formation of the hydroxymethyl phenols and the self-assembly of the PF and block copolymer template are mostly induced by the high acidic condition. The resulting carbon exhibits a highly organized hexagonal mesostructure once the template is removed. It has a surface area of 760 m^2g^{-1}, a large pore volume of 0.64 cm^3g^{-1}, and a uniform pore size of 3.32 nm [8]. According to Marta et al., the curing of resol resin at high temperatures occurs in a relatively short time. As a result, there is an insignificant relationship between the composition of pyrolyzate and the duration of the curing process. The number of low-volatile components in pyrolysis products is affected by increasing the temperature in the range of 650-900 °C [9]. To produce lighter fuel oil, Kasar et al. investigated the catalytic co-pyrolysis of Bakelite and refinery residual fuel oil using the ZSM-5 catalyst. They found that when the separate feedstocks are merged, the degradation of the individual feedstocks, particularly Bakelite, is enhanced, showing a synergistic impact on mixing. Furthermore, the majority of the degradation occurs between 250 °C and 400 °C [10].

A few scholars used various kinetics models to study the kinetics parameters of Bakelite's thermal degradation. To separate the overall decomposition rate of the phenolic binder in a silica-phenolic ablator into its individual reactions, Bishop and Mlnkowycz provided a test procedure and method of analysis. Then for these separate reactions, the Arrhenius rate equations are determined and a proposed reaction mechanism is used to predict the decomposition rate of the phenolic for both constant and varying test temperatures [11]. Haiyun Jiang et al. investigated the kinetics of the pyrolysis process of PF resin using the TGA technique. The kinetic parameters of thermal degradation are determined using model-free methods, and the reaction models are developed using linear regression. To reduce the error caused by the choice of the reaction model, 36 typical mechanism functions are provided for the purpose of estimating the probable mechanism. There are three consecutive and overlapped regions in the pyrolysis process. Each stage's apparent activation energy is 222.73, 271.70, and 305.14 KJ/mol, respectively, with pre-exponential factors of 1.19×10^9, 4.02×10^6, and 3.60×10^7 min^{-1} [12].

However, an extensive study of thermal degradation mechanism, kinetics, co-pyrolytic synergy, and thermodynamics of waste Bakelite samples using a wide variety of established kinetic models is missing in the literature. Again, in all previous works, pure PF resin is taken for thermal degradation study, but in actual practice 100% pure resin is not used for the production of final products. Some other ingredients, including fillers, coloring materials, lubricants, etc. are mixed with pure PF resin to get the desired product quality and aesthetics. Thus, the presence of all these additives would definitely change the thermal degradation behavior and kinetics of PF resin. To build a more efficient thermal modification system and forecast a solid-state process, additional study is needed to have a comprehensive grasp of pyrolysis kinetics.

In the present work, discarded electrical appliances. like switches, three-pin plugs, are used as a source of Bakelite. Such discarded electrical appliances have undergone aging during their prolonged uses due to exposure to thermal stress and other environmental conditions. Thus, the thermal degradation behavior of such samples needs to be studied to utilize them by a thermal recycling technique. This also necessitates a thorough kinetics and thermodynamics investigation. Model fitting, model-free, and Master plot (MP) approaches have been used to conduct the kinetic analysis. And, using recognized thermodynamic equations, thermodynamic parameters (ΔG, ΔS, and ΔH) are computed.

EXPERIMENTAL

1. Material

The waste electrical appliances are used as a source of Bakelite. They are crushed into small pieces manually and then ground into the powdered form of about 1 mm size by a household grinder.

2. Methods

2-1. Analysis of Bakelite Sample

The percentage of moisture, volatile matter, fixed carbon, and ash content of Bakelite samples is estimated by using American Society for Testing Materials (ASTM) D 4442, ASTM D 3172, ASTM D 3177, and ASTM D 3175 standard procedures, respectively, in the proximate analysis. CHNS elemental analyzer is used to determine the Bakelite's elemental composition (C, H, N, S, O) (Variael CUBE, Germany). X-ray fluorescence (XRF) spectrometer of model PW2400 of Philips made with microprocessor-controlled HT generator, an X-ray tube of rhodium anode, scintillation detector with a current 40 MA and voltage 40 MV, Goniometer (slewing speed 40° 2θ/s and scanning speed 0.0001° to 2° 2θ/s), 300 μm collimator, is used to determine the elemental composition of the Bakelite. To determine the functional group composition of the Bakelite, the Fourier transformed infrared (FTIR) spectrum is taken in a Bruker Alpha FTIR spectrophotometer with a spectral range of 500-4,000 cm^{-1} and a resolution of 2 cm^{-1}, equipped with a DLATGA detector, Universal ZnSe ATR, gold-coated mirrors, ZnSe beam splitter, and window and OPUS software.

2-2. TG-DTG and DSC Analysis

A Pyris Simultaneous Thermal Analyzer 8000 is used for the TG/DTG and DSC analysis of the powdered discarded Bakelite sample. During analysis, generally, approximately 4-14 mg of sample is taken in a ceramic pan in each trial. In this work, nearly 9.4±0.35-milligram sample was taken in the crucible placed in the inert nitrogen gas atmosphere at approximately 19.8 ml/minute gas flow for a temperature range of 30-1,000 °C at five different heating rates (5, 10, 20, 30 and 50 °C/min.). All the calculations parts were done by Microsoft Office Excel 2019 and graphs were drawn and analyzed by Origin software 8.5 ®.

2-3. Kinetic and Thermodynamic Analysis

The rate equation for the solid-state reaction may be represented as:

$$\frac{d\alpha}{dt} = Ae^{(-Ea/RT)} \cdot f(\alpha) \quad (1)$$

where, $\frac{d\alpha}{dt}$=rate of reaction, Ea=activation energy, R=gas constant,

T=temperature, f(α)=function of α whose value will vary from model to model

A=pre-exponential frequency/Arrhenius factor, α=conversion fraction

$$\text{Mathematically, } \alpha = \frac{W_0 - W_t}{W_0 - W_f} \tag{2}$$

where, W_0=initial weight, W_t=weight at 't' time, W_f=final weight

Eq. (1) can be transformed into a non-isothermal rate equation with a function of temperature by

$$\frac{d\alpha}{dT} = \frac{d\alpha}{dt}\frac{dt}{dT} = \frac{1}{\beta}\frac{d\alpha}{dt} \tag{3}$$

Where, $\beta = \frac{dT}{dt}$=heating rate

From Eqs. (1) and (3),

we get,

$$\frac{d\alpha}{dT} = \frac{A}{\beta} e^{-Ea/RT} f(\alpha) \tag{4}$$

$$\Rightarrow \frac{d\alpha}{f(\alpha)} = \frac{A}{\beta} e^{-Ea/RT} dT \tag{5}$$

Eq. (5) is the differential form of the rate law for solid-state kinetics

Now integrating both sides of Eq. (5) then,

$$\int_0^{\alpha} \frac{d\alpha}{f(\alpha)} = \frac{A}{\beta}\int_0^{T} e^{-Ea/RT} dT$$

$$\Rightarrow g(\alpha) = \frac{A}{\beta}\int_0^{T} e^{-Ea/RT} dT \tag{6}$$

Where, $g(\alpha) = \int_0^{\alpha} \frac{d\alpha}{f(\alpha)}$

Eq. (6) is the integral form of the rate law.

For different model fitting methods, Table S1 [13] is used for the f(α) value.

The kinetics analysis can be determined by a model-free method which is classified into two methods, the differential and integral, by using some integral approximation.

The Friedman differential method belongs to Eq. (7) [13] which can be directly derived by using Eq. (6)

$$\ln\left(\frac{d\alpha}{dT}\right) = \ln[A(1-\alpha)] - \frac{Ea}{RT} \tag{7}$$

So, the plot between $\ln\left(\frac{d\alpha}{dT}\right)$ and 1/T should give a curve with slope and intercept $-E_a/R$ and, respectively.

On the other hand, the integral method can be shown its validity by solving Eq. (6). After solving Eq. (6), Eq. (8) is derived.

$$g(\alpha) = \int_0^{\alpha} \frac{d\alpha}{f(\alpha)} = \frac{A}{\beta}\int_0^{T} e^{(-Ea/RT)} dT = \frac{AEa}{\beta R} p(x) \tag{8}$$

Where, x=Ea/RT

Ea and A are calculated using the integral iso-conversion methods like KAS, FWO, STR, LTA, and VYZ methods, as well as the differential iso-conversional FRM method. The above integral iso-conversion method has a definite empirical approximation p(x) value, and by putting the empirical approximation value for KAS, FWO, and STR methods, the kinetic equations are derived. Differential FRM and LTA integration methods have no approximation, while VYZ method is a non-linear iso-conversional method. All the suitable equations are tabulated in Table S2 and Table S3 [13].

Here, the order of reaction is found at 150 °C, 200 °C, 250 °C, 300 °C, 350 °C, 400 °C and 450 °C for 5, 10, 20, 30 and 50 °C/min heating rate. The order of the reaction is calculated by AVM theory [13]. According to this theory,

$$\ln(-\ln(1-\alpha)) = \ln A - \frac{Ea}{RT} - n\ln\beta \tag{12}$$

where, T=Temperature, α=Degree of conversion, β=Heating rate, n=Order of reaction, A=Arrhenius constant, R=Universal gas constant, and Ea=Activation Energy

In this method, a graph is drawn between lnβ along X-axis and $\ln(-\ln(1-\alpha))$ along Y-axis at constant temperature. The order of the reaction is equal to the slope of the curve as per Eq. (12).

The value of ΔG, ΔH, and ΔS can be calculated by using Eqs. (13), (14), (15), Kissinger model, and DTG graph [13].

$$\Delta G = Ea + RT_m \ln\left(\frac{k_b T_m}{hA}\right) \tag{13}$$

$$\Delta H = Ea - RT_m \tag{14}$$

$$\Delta S = \frac{\Delta H - \Delta G}{T_m} \tag{15}$$

where, K_b=Boltzmann constant (1.381×10^{-23} J/K), h=Planck's constant (6.626×10^{-34} J/s), A=pre-exponential factor (min^{-1}), T_m=peak temperature at the particular heating rate in the DTG curves, Ea=activation energy calculated by Kissinger method.

RESULTS AND DISCUSSION

1. Characterization of Bakelite Sample

According to the proximate analysis, Bakelite contains 68.22%

Table 1. XRF analysis of discarded Bakelite and its char

Components	Material	
	Discarded Bakelite (weight%)	Char (weight%)
SiO_2	54.463	54.545
Al_2O_3	30.326	29.560
BaO	4.590	4.530
CaO	2.061	2.050
ZnO	1.942	1.987
Fe_2O_3	1.554	1.654
K2O	1.132	1.510
TiO_2	1.466	1.567
Cr_2O_3	0.944	0.970
P_2O_5	0.618	0.692
MnO	0.502	0.521
CuO	0.188	0.189
SrO	0.111	0.121
Eu_2O_3	0.103	0.104

volatile compounds, 3.24%, moisture content, 6.82% ash content, and 21.72% fixed carbon. Due to high % volatile content and low % moisture and ash content, the discarded Bakelite can be used as potential feedstock in the pyrolysis process. High % fixed carbon also promotes the conversion of such wastes into valuable carbonaceous products. According to ultimate analysis, the discarded Bakelite contains the highest carbon of 68.04% followed by 14.78% oxygen, 5.09% hydrogen, no nitrogen and sulfur. From Table 1, the Bakelite and char contain SiO_2, Al_2O_3, and BaO as major components.

From Fig. S1, it is seen that the peak at 3,321, 2,920, 1,640, 1,551, 1,383, 776, and 609 cm^{-1} indicates the presence of normal polymeric O-H stretching, C-H stretching, aryl-substituted C=C stretching, C-C=C aromatic ring stretching, C-H bending, -CH_2 rocking vibration, and C-H out of plane bending vibration, respectively. The peak at 776 cm^{-1} also indicates the presence Si-O-Al, while the peak at 1,041 cm^{-1} indicates the presence of Si-O stretching, which confirms the presence of silicate ion and, subsequently, indicates the presence of organic siloxane or silicone (Si-O-Si). From the above discussion, it is clear that the sample collected from the electrical waste switches, plugs, etc., contains Bakelite as a main raw material with a little filer like SiO_2 and Al_2O_3.

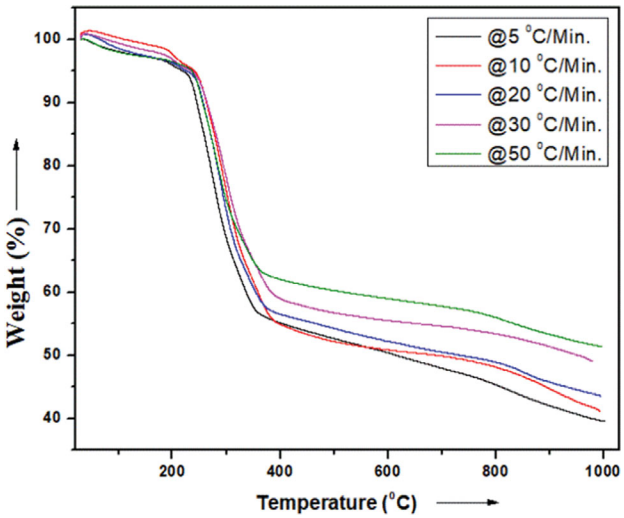

Fig. 1. TG curves of discarded Bakelite sample.

2. Thermal Degradation Behavior

The thermal degradation behavior of the discarded bakelite at different heating rates is shown in Figs. 1 and 2. There are four

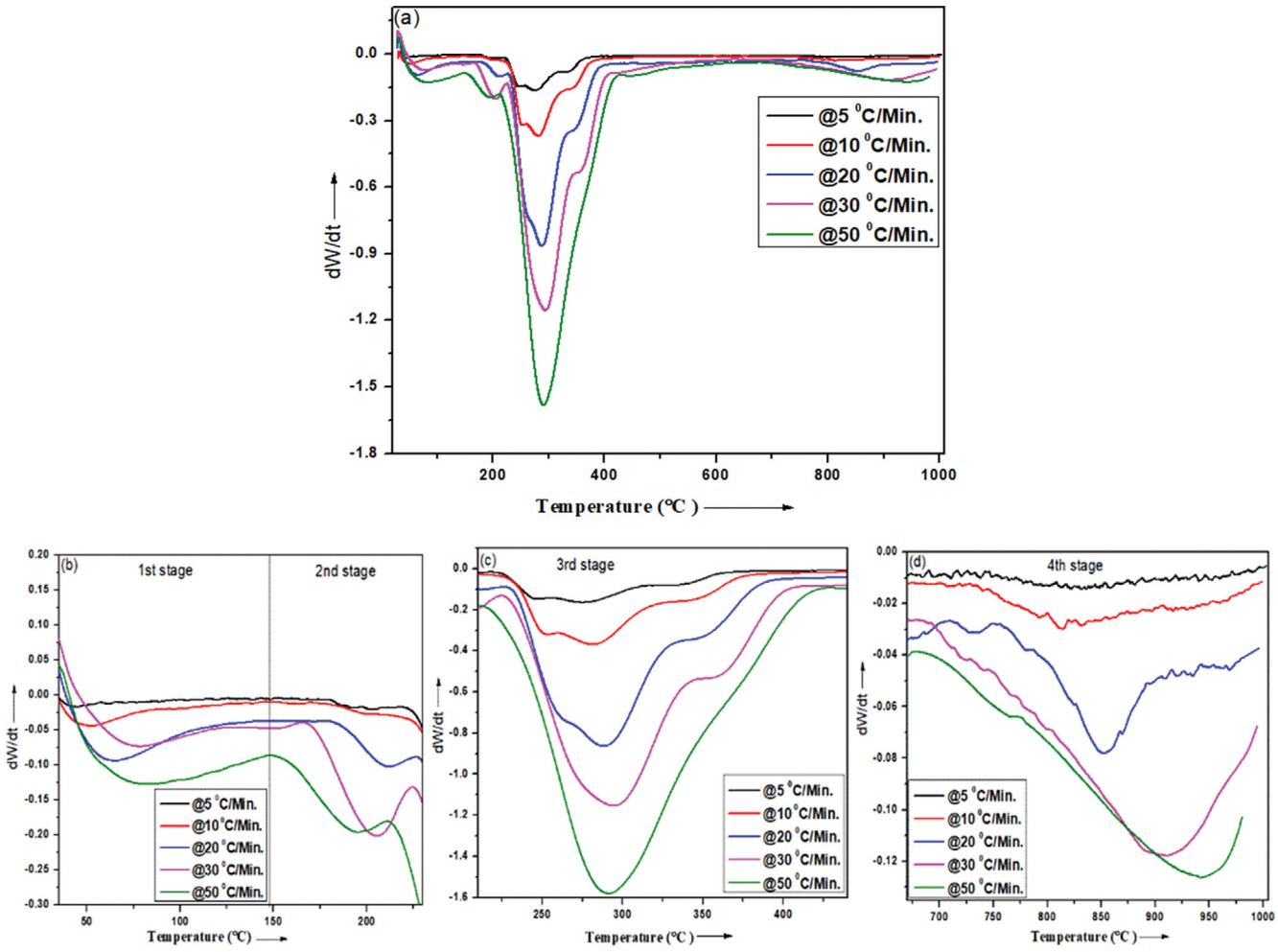

Fig. 2. (a) DTG curve of discarded Bakelite (30-1,000 °C), (b) 1st stage and 2nd stage, (c) 3rd stage, (d) 4th stage.

Table 2. Weight loss of discarded Bakelite at different stages

Heating rate (°C/Min.)	First stage			Second stage			Third stage			Fourth stage			Total weight loss (%)
	T_i	T_f	W	T_i	T_f	W	T_i	T_f	W	T_i	T_f	W	
5	30	181	3.47	181	226	1.88	226	360	37.86	360	1,000	17.13	60.34
10	30	183	1.48	183	228	2.82	228	381	39.50	381	1,000	15.14	58.94
20	30	185	3.01	185	231	2.49	231	392	37.70	392	1,000	13.75	56.95
30	30	167	2.40	167	225	2.10	225	405	36.80	405	1,000	9.70	51
50	30	152	2.70	152	211	1.30	211	424	34.63	424	1,000	10.07	48.7

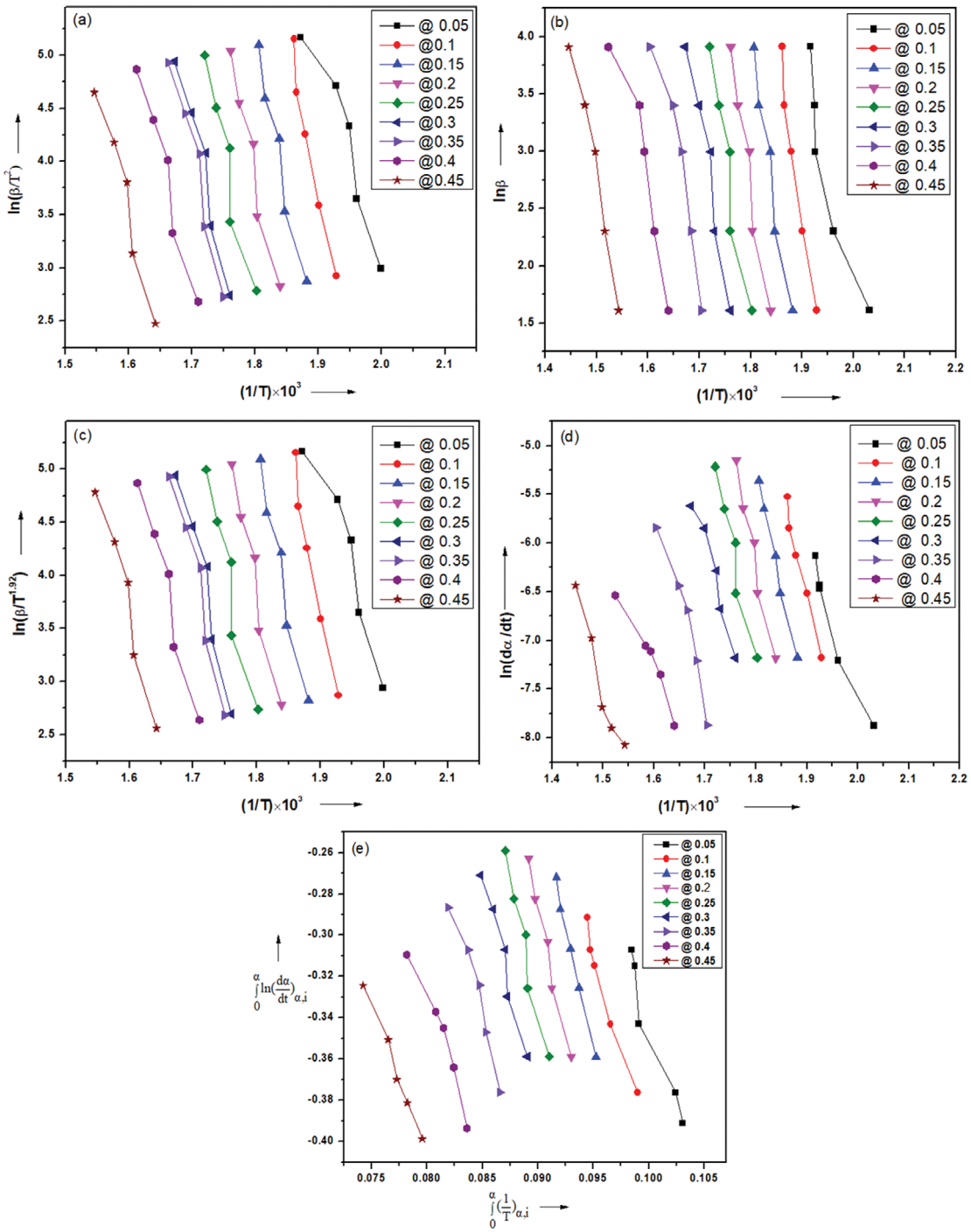

Fig. 3. Model free method showing (a) KAS, (b) FWO, (c) STR, (d) FRM, (e) LTA.

stages of the thermal degradation of the discarded bakelite in the temperature range 30-1,000 °C. Table 2 summarizes the initial temperature (T_i), final temperature (T_f) and % weight loss (W) at different stages.

The first stage varies from 30 to 185 °C at various heating rates, with the maximum 3.47% mass loss occurring at 5 °C/minute. In this stage, the sample attain the glass transition temperature nearly at 55 °C where it is softened [14]. Between 70-110 °C, the discarded Bakelite molecules lose the adsorbed water molecules [10,15] while at 74.4 °C, the volatiles substances are released from the discarded Bakelite [15] and subsequently, it gels at 97 °C [12]. The second stage ranges from 185 to 231 °C in which the maximum 2.82% mass loss occurs at 10 °C/minute. In this stage, water molecules form due to the random degradation and cross-linking of Bakelite molecules (200-300 °C) [16]. The formation of phenol derivatives, heavier aromatic species, and elimination of water (227-577 °C) starts from the second stage and continues up to the last stages [17]. The third stage ranges from 231 to 424 °C with a maximum of 39.5% weight lost at a 10 °C/min heating rate. Below 350 °C, the oligomer in the original resin is evaporated [18]. Ouchi reported that up to 300 °C, there is no change in the linear structure of Bakelite due to crossing-linking [19]. Costa et al. and Wang et al. informed that the disintegration of the polymeric system and elimination of various volatiles, water, and unreacted oligomers take place beyond 350 °C [18,20]. Chen et al. reported the major degradation of the polymer and loss of water takes place between 400-600 °C [17]. However, the carbonization of discarded Bakelite begins at 350 °C and continues up to the end of the process [20]. The fourth stage ranges from 424 to 1,000 °C with a maximum of 17.13% weight lost at 5 °C/min. heating rate. Benzene, toluene, and xylene are formed between 427 and 577 °C [21], while CO and CO_2 are evolved at 450 °C [16]. Aromatic hydrogen is released at above 500 °C [19], while Tar and CH_4 are formed at 550 °C and 625 °C, respectively [16]. The formation of methanol, phenol, 2,6-xylenol, 2,4-xylenol, and, 2,4,6-Trimethylphenol takes place at 650 °C. At 750 °C, naphthalene, biphenyl, dibenzofurans, fluorene, phenanthrene, and anthracene are formed [20]. After 750 °C, the above reaction continues with the increase in temperature and causes slow weight loss up to 1,000 °C, which is shown in Fig. 1 and Fig. 2. Finally, it may be concluded that the substance collected at 1,000 °C is a mixture of more amount of char with some filler like SiO_2, Al_2O_3, BaO, CaO, ZnO, etc. (Table 1). Table 2 shows that the total weight loss ranges from 49-61% in the 30-1,000 °C temperature range at various heating rates. In Fig. 2, the peak temperature rises from 44 °C to 84 °C, 195 °C to 210 °C (with modest deviations at 30 °C/min. and 50 °C/min. heating rate), 275 °C to 295 °C, and 813 °C to 943 °C in the first stage, second stage, third stage and fourth stage, respectively, with an increase in the heating rate from 5 to 50 °C/min.

Table 3. Results of different iso-conversional methods

α	KAS				FWO				STR			
	Ea (KJ/mol)	A (min^{-1})	R^2	Error (%)	Ea (KJ/mol)	A (min^{-1})	R^2	Error (%)	Ea (KJ/mol)	A (min^{-1})	R^2	Error (%)
0.05	145.442	2.021×10^{21}	0.907	3.859	145.876	6.963×10^{14}	0.906	3.572	148.440	6.345×10^{14}	0.907	1.877
0.1	257.484	1.082×10^{32}	0.949	6.404	266.261	8.508×10^{25}	0.952	3.213	263.347	2.570×10^{25}	0.955	4.272
0.15	240.344	3.896×10^{29}	0.942	4.984	249.363	4.231×10^{23}	0.947	1.418	245.601	1.027×10^{23}	0.948	2.905
0.2	237.534	4.958×10^{28}	0.932	4.027	246.770	6.404×10^{22}	0.937	0.295	242.545	1.371×10^{22}	0.937	2.002
0.25	226.320	1.199×10^{27}	0.909	4.305	235.757	1.929×10^{21}	0.909	0.314	231.120	3.709×10^{20}	0.909	2.275
0.3	214.051	2.547×10^{25}	0.931	1.766	223.745	5.168×10^{19}	0.936	2.682	217.820	7.493×10^{18}	0.930	0.037
0.35	213.994	1.677×10^{25}	0.931	1.748	189.552	1.378×10^{16}	0.909	12.970	217.740	5.208×10^{18}	0.930	0.028
0.4	193.009	5.532×10^{22}	0.935	1.777	164.850	2.580×10^{13}	0.905	16.107	196.497	2.068×10^{16}	0.938	0.002
0.45	193.949	1.052×10^{22}	0.935	2.095	201.166	2.050×10^{15}	0.967	1.548	198.039	5.072×10^{15}	0.934	0.031
Avg.	213.570	1.21×10^{31}	0.930	0.178	213.705	9.508×10^{24}	0.930	0.115	217.906	2.87×10^{24}	0.932	1.849

α	FRM				LTA				VYZ
	Ea (KJ/mol)	A (min^{-1})	R^2	Error (%)	Ea (KJ/mol)	A (min^{-1})	R^2	Error (%)	Ea (KJ/mol)
0.05	119.872	1.912×10^{9}	0.928	20.762	133.623	1.404×10^{10}	0.901	11.672	151.28
0.1	188.950	9.144×10^{15}	0.970	31.316	146.285	1.172×10^{5}	0.957	46.825	275.1
0.15	200.641	4.513×10^{16}	0.985	20.680	196.576	4.402×10^{4}	0.989	22.287	252.95
0.2	214.270	3.482×10^{17}	0.953	13.426	207.559	2.731×10^{3}	0.972	16.138	247.5
0.25	200.423	7.205×10^{15}	0.920	15.255	207.617	3.254×10^{2}	0.940	12.213	236.5
0.3	154.817	1.960×10^{11}	0.938	28.950	178.493	2.834×10^{1}	0.942	18.085	217.9
0.35	162.707	2.236×10^{11}	0.922	25.295	159.887	0.670×10^{1}	0.939	26.590	217.8
0.4	91.101	4.676×10^{4}	0.932	53.638	124.569	0.150×10^{1}	0.927	36.606	196.5
0.45	149.362	5.145×10^{8}	0.915	24.603	118.583	0.090×10^{1}	0.985	40.140	198.1
Avg.	164.683	4.55×10^{16}	0.941	23.027	163.688	1.756×10^{9}	0.950	23.492	213.95

From the DSC plot (Fig. S2) at 30 °C/min. heating rate, the glass transition temperature of the discarded Bakelite is 54.95 °C, which resembles that of the glass transition temperature of pure phenol-formaldehyde [14]. From the glass transition temperature, it confirms the sample to be made of Bakelite.

3. Kinetics Analysis

3-1. Model-free Method

The conversion value (α), which ranges from 0.05 to 0.45 with a difference of 0.05, is taken to plot the linear graphs for different linear iso-conversional methods (Fig. 3).

The values of Ea, A, and R^2 at different conversions are evaluated through the above methods (Table S2 and S3) and are given in Table 3.

3-1-1. Calculation of Activation Energy

The values of activation energy obtained at different conversions and at different heating rate are not the same. This might be due to the presence of filler and the complex nature of thermal degradation of discarded Bakelite. Table 3 shows that the Ea value is low at 0.05 conversion. This conversion is related to the loss of adsorbed water and volatiles, which needs less energy. But at the subsequent conversion, i.e., at 0.1 conversion, the Ea value is high. This is because of the random degradation with the cross-linking process for the formation of water molecules. The value of Ea starts to decrease after 0.1 conversion up to 0.40 conversion except for a slight deviation in the FRM and LTA method. This is because this conversion range is related to the evaporation of oligomer in the original resin, water molecules etc. With the exception of the LTA method, after 0.40 conversion, the value of Ea suddenly starts to increase at 0.45 conversion, as it deals with the commencement of the disintegration of the polymeric system and the elimination of various volatiles, water molecules, etc. The Ea values may increase up to that next conversion where the disintegration of the polymeric system will be complete. It can be seen that the conversion rate changes as the heating rate increases. The conversion extends up to 0.6, 0.45, 0.55, 0.55 and 0.5 at 5, 10, 20, 30 and 50 °C/min, respectively, because the conversion decreases with the increase of heating rate. Here deviation is seen at 10 °C/min. After 0.45 conversion, no subsequent conversion is found at 10 °C/min. heating rate between 30-1,000 °C temperature. This irregular conversion may be due to the presence of a non-uniform amount of filler like SiO_2, Al_2O_3, BaO, CaO, and ZnO (Table 1). From Table 3, it is concluded that a large deviation is found in the FRM and LTA method, and less deviation is found in the STR method during the calculation of the value of Ea as compared to the other three methods: KAS, FWO, and VYZ. FRM is a differential iso-conversional method, while LTA is an integrational iso-conversional method and both have no approximation value, while the other three methods, KAS, FWO, and STR, are integrational iso-conversional methods with approximation. This might explain why the average value of Ea computed by the FRM method and LTA method differs significantly from the other three method (KAS, FWO, and STR). The average value of Ea determined by the KAS, FWO, and VYZ techniques is virtually identical, whereas the average value of Ea obtained by the STR method is somewhat lower. The average value of Ea (213.95 KJ/mol) estimated using the VYZ method for the thermal degradation of discarded Bakelite is accepted as a more accurate value because it is a non-linear iso-conversional method. The error (%) in the Ea value can be calculated by Eq. (16):

$$\text{Error (\%)} = \left[\frac{E_{VYZ} - E_{KAS}, E_{FWO}, E_{STR}, E_{FRM}, E_{LTA}}{E_{VYZ}}\right] \times 100 \qquad (16)$$

From Table 3, it is seen that the mean error of Ea in percentage value, which was calculated for various linear methods like FWO, KAS, STR, FRM, and LTA based on the non-linear method (VYZ), results are changed from 0.115% to 23.492%, and increased in the order of FWO<KAS<STR<FRM<LTA. Finally, the average Ea value for the thermal degradation of discarded Bakelite waste is determined to be 213 KJ/mol. However, the activation energy calculated by the Kissinger method is 105.492 KJ/mol.

Fig. S3 is obtained by taking conversion (α) on the X-axis and Ea value on the Y-axis, and it shows that there is a predictable pattern in the change of Ea value with respect to conversion in various iso-conversional methods such as KAS, FWO, STR, FRM, LTA, and VYZ. The value of Ea varies with the amount of mass lost during thermal degradation, suggesting that the PF resin degradation belongs to a complicated mechanism [15].

3-1-2. Calculation of Arrhenius Factor

Various conversions resulted in different values of A. This might be as a result of the fillers present and the complex nature of the thermal degradation processes of discarded Bakelite. From Table 3, it is observed that except LTA method, in KAS, FWO, and STR methods, the value of A is low at the beginning, i.e., 0.05 conversion, then the value of A increases up to 0.45 conversion. At 0.05 conversion, surface reactions like dehydration and devolatization take place. On the other hand, the value of A calculated by FRM

Table 4. Results of reaction mechanism by the model fitting method

Reaction model	E_a (KJ/mol)	A (min^{-1})	R^2
P_2	26.018	0.117×10^9	0.908
P_3	17.345	0.015×10^9	0.909
P_4	13.008	0.005×10^9	0.900
$P_{3/2}$	78.052	$6{,}279.9\times10^9$	0.904
A_2	33.827	9.1×10^9	0.970
A_3	22.551	0.075×10^9	0.970
A_4	16.914	0.018×10^9	0.970
R_2	58.363	8.727×10^{10}	0.934
R_3	61.070	12.129×10^{10}	0.946
D_1	104.070	1.174×10^{15}	0.908
D_2	111.255	4.026×10^{15}	0.918
D_3	122.138	16.129×10^{15}	0.946
D_4	114.690	2.23×10^{15}	0.928
F_0	52.035	3.081×10^{10}	0.908
F_1	67.654	2.149×10^{12}	0.970
$F_{1.5}$	29.338	1.722×10^{12}	0.918
F_2	96.502	4.697×10^{15}	0.978
$F_{2.5}$	114.256	5.192×10^{17}	0.954
F_3	133.185	7.783×10^{19}	0.927
F_4	172.750	2.660×10^{24}	0.909
F_5	213.914	1.360×10^{29}	0.915

for different conversions (0.05-0.45) does not show the regular trend, but in the LTA method the value of A decreases from 0.05 to 0.45 conversion. The average value of A determined by each method is different from one another. However, the average value of A (4.55×10^{16} min^{-1}) calculated by FRM method for different conversions is nearly equal to the value of A (4.13×10^{16} min^{-1}) calculated by the Kissinger method. Finally, it is concluded that the value of A for the thermal degradation of discarded Bakelite may be in the range of 4.13×10^{16} min^{-1}-4.55×10^{16} min^{-1}.

3-2. Model Fitting Method

The values of Ea, A, and R^2 are also determined by using model-fitting methods at different heating rates, and the average value of Ea, A, and R^2 are given in Table 4.

Only F_5 models (213.914 KJ/mol) show the best agreement in Ea value calculation with the Ea value calculated by the VYZ method (213.95 KJ/mol) and slightly deviate from KAS (213.57 KJ/mol), FWO (213.705 KJ/mol) and STR (217.9 KJ/mol). Table 4 shows that the value of Ea ranges from 13 KJ/mol to 78 KJ/mol, 58 KJ/mol to 61 KJ/mol, 104 KJ/mol to 122 KJ/mol, and 29 KJ/mol to 213 KJ/mol for the nucleation model, geometrical contraction model, diffusion model, and order-based model, respectively. Similarly, A value ranges from 0.005×10^9 min^{-1} to $6{,}279.9\times10^9$ min^{-1}, 8.727×10^{10} min^{-1} to 12.129×10^{10} min^{-1}, 1.174×10^{15} min^{-1} to 16.129×10^{15} min^{-1} and 3.081×10^{10} min^{-1} to 1.36×10^{29} min^{-1} for the nucleation model, geometrical contraction model, diffusion model, and order-based model, respectively. Similarly, the R^2 value ranges from 0.90 to 0.97, 0.934 to 0.946, 0.908 to 0.946 and 0.908 to 0. 978 for the nucleation model, geometrical contraction model, diffusion model and order-based model, respectively. From the above discussion, it is clear that there is no correlation between any model in terms of Ea, A, and R^2 values. However, the R^2 value (0.97) for A_2, A_3, and A_4 nucleation models is the same as the R^2 value for F_1 order-based model. This variation in data may be due to the limitation in the model fitting model. Furthermore, the master plot (MP) approach is used to validate the model fitting models. According to ICTAC and kinetic committee, MP gives a more precise and well-defined estimation of the reaction model. The master plot (Fig. S4) is drawn by taking the $f(\alpha)/f(0.5)$ on the Y-axis while conversion (α) on the X-axis. According to Table S1, the function $f(\alpha)$ is dependent on the reaction mechanism, and f(0.5) is dependent on the reaction mechanism when $\alpha=0.5$. From the master plots (Fig. S4), it is seen that the master plot for the order-based model shows a well-defined trend which must be given a more precise and well-defined estimation of the reaction model. From the master plot Fig. S4(d), it is seen that all curves show good trend variation with respect to $f(\alpha)/f(0.5)$ and conversion (α). So, it is concluded that the reaction mechanism must belong to the order-based model.

3-3. Reaction Mechanism

The mechanism of thermal degradation of discarded Bakelite can be explained by the F_5 order-based model. This is because the Ea value determined by the KAS (213.570 KJ/mol), FWO (213.705 KJ/mol), and VYZ (213.95 KJ/mol) methods is approximately equivalent to the Ea value calculated by the order-based F_5 model (213.914 KJ/mol). However, the Ea value calculated by the order-based F_5 model is nearly 4 units less than the Ea value calculated by the STR (217.9 KJ/mol) method. From the above discussion, it is concluded that the thermal degradation of discarded Bakelite follows the F_5 order-based mechanism with the values of R^2, Ea and A found to be 0.93, 213 KJ/mol, and 4×10^{16} min^{-1} respectively.

Table 5. Thermodynamic parameters at a different heating rate

Heat rate (°C/min)	ΔG (KJ/mol)	ΔH (KJ/mol)	ΔS ($JK^{-1}mol^{-1}$)
5	554.186	100.901	-820.870×10^{-3}
10	558.126	100.861	-820.942×10^{-3}
20	562.838	100.814	-821.027×10^{-3}
30	563.873	100.803	-821.045×10^{-3}
50	564.694	100.795	-821.060×10^{-3}
Average	560.743	100.835	-820.989×10^{-3}

3-4. Reaction Order Analysis

In this work, Fig. S5 was obtained by taking $\ln\beta$ on the X-axis and $\ln(-\ln(1-\alpha))$ on the Y-axis at 5, 10, 20, 30, and 50 °C/min heating rate at a constant temperature. The order of the reaction at different temperatures is summarized in Table S4. The order of the reaction rises at 250 °C, decreases up to 400 °C, and then increases at 450 °C, as shown in Table S4.

4. Thermodynamic Parameter

The values of ΔG, ΔH, and ΔS are calculated by using Eqs. (13), (14), and (15) at different heating rates respectively, and the values are listed in Table 5.

In this work, the values of ΔG, and ΔS increase, but ΔH decreases by increasing the heating rate. However, the increase of ΔS and decrease of ΔH is not significant. The positive value of both ΔG and ΔH and the negative value of ΔS shows that the reaction is non-spontaneous at all temperatures. The positive value of ΔH demonstrates that the thermal degradation of discarded Bakelite is an endothermic reaction, indicating that considerable energy is required for the reaction to occur.

CONCLUSION

This work performed non-isothermal pyrolysis of discarded Bakelite at various heating rates, and the pyrolysis kinetics was examined using several types of model-free and model fitting methods. Bakelite pyrolysis was found to occur in four steps. The average values of activation energy calculated from KAS, FWO, STR, and VYZ models were found almost the same. The thermal degradation of discarded Bakelite follows an F_5 order-based mechanism with an average activation energy of 213 KJ/mol. The accuracy of the mechanism was also confirmed by the master plots. The value of the Arrhenius constant was found to be 4×10^{16} min^{-1}. The order of reaction calculated by the AVM theory ranged from 0.016 to 0.349 depending upon the temperatures. The average thermodynamic parameters such as ΔG, ΔH, and ΔS were 560.743 KJ/mol, 100.835 KJ/mol, and -820.989×10^{-3} $JK^{-1}mol^{-1}$, respectively, and are almost the same at different heating rates.

SUPPORTING INFORMATION

Additional information as noted in the text. This information is

available via the Internet at http://www.springer.com/chemistry/journal/11814.

REFERENCES

1. https://en.wikipedia.org/wiki/Thermosetting_polymer#Applications, date of access: 05/09/2022.
2. L. Xu, Q. q. Zhong, Q. Dong, L. y. Zhang and Z. Fang, *J. Anal. Appl. Pyrol.*, **142**, 104663 (2019).
3. Phenolic Resins Market Size, Share & Trends Analysis Report by Product (Novolac, Resol), By Application (Wood Adhesives, Molding, Insulation, Laminates, Paper Impregnation, Coatings), And Segment Forecasts, 2020-2025, Report ID: 978-1-68038-271-6,https://www.grandviewresearch.com/industry-analysis/phenolic-resins-market/segmentation,date of access:08/09/2022.
4. N. Usahanunth and S. Tuprakay, *Case Stud. Constr. Mater.*, **6**, 120 (2017).
5. T. Horikawa, K. Ogawa, K. Mizuno, J. Hayashi and K. Muroyama, *Carbon*, **41**, 465 (2003).
6. T. Yamamoto, T. Ohmori and Y. Kim, *Carbon*, **48**, 912 (2010).
7. E. Fitzer, W. Schaefer and S. Yamada, *Carbon*, **7**, 643 (1969).
8. M. Xie, H. Dong, D. Zhang, X. Guo and W. Ding, *Carbon*, **49**, 2459 (2011).
9. M. Sobera and J. Hetper, *J. Chromatogr. A*, **993**, 131 (2003).
10. P. Kasar and M. Ahmaruzzaman, *J. Sci. Ind. Res.*, **78**, 426 (2019).
11. W. M. Bishop and W. J. Minkowycz, *AIAA J.*, **11**(4), 438 (1973).
12. H. Jiang, J. Wang, S. Wu, B. Wang and Z. Wang, *Carbon*, **48**, 352 (2010).
13. A. Sahoo, S. Kumar and K. Mohanty, *Renew. Energy*, **165**, 261 (2021).
14. Z. Li, W. Zhou, L. Yang, P. Chen, C. Yan, C. Cai, H. Li, L. Li and Y. Shi, *Polymer*, **11**, 1 (2019).
15. M. V. Alonso, M. Oliet, J. C. Domınguez, E. Rojo and F. Rodrıguez, *J. Therm. Anal. Calorim.*, **105**, 349 (2011).
16. M. A. Serio, S. Charpenay, R. Bassilakis and P. Solomon, Conference: ACS Divsion of Fuel Chemistry Preprints; Atlanta, GA, **36**(2) 664 (1991)
17. R. Chen, X. Xu, S. Lu, Y. Zhang and S. Lo, *Energy Convers. Manag.*, **165**, 555 (2018).
18. L. Costa, L. R. d. Montelera, G. Camino, E. D. Weil and E. M. Pearce, *Polym. Degrad. Stabil.*, **56**, 23 (1997).
19. K. Ouchi, *Carbon*, **4**, 59 (1966).
20. J. Wang, H. Jiang and N. Jiang, *Thermochim. Acta*, **496**, 136 (2009).
21. H. W. Wong, J. Peck, R. E. Bonomi, J. Assif, F. Panerai, G. Reinisch, J. Lachaud and N. N. Mansour, *Polym. Degrad. Stabil.*, **112**, 122 (2015).

Supporting Information

Pyrolysis kinetics and thermodynamics of discarded Bakelite

Pabitra Mohan Mahapatra*, Achyut Kumar Panda*,†, Sahin Ahmed, and Sachin Kumar*****

*Department of Chemistry, Veer Surendra Sai University of Technology, Burla, Odisha, India, PIN 768018
**Department of Civil Engg., Veer Surendra Sai University of Technology, Burla, Odisha, India, PIN 768018
***Department of Energy Engineering, CoE-GEET, Central University of Jharkhand Brambe, Ranchi, India-835205
(*Received 20 July 2022 • Revised 4 October 2022 • Accepted 26 October 2022*)

Table S1. Differential and integral forms of different kinetic models of the solid-state pyrolysis

Kinetic model	Notation	Differential form (f(α))	Integral form (g(α))
Nucleation model			
Power Law	P_2	$2\alpha^{1/2}$	$\alpha^{1/2}$
	P_3	$3\alpha^{2/3}$	$\alpha^{1/3}$
	P_4	$4\alpha^{3/4}$	$\alpha^{1/4}$
	$P_{3/2}$	$(3/2)\ \alpha^{1/3}$	$\alpha^{2/3}$
Avrami Erofeyev	A_2	$2(1-\alpha)\ [-\ln(1-\alpha)]^{1/2}$	$[-\ln(1-\alpha)]^{1/2}$
	A_3	$3(1-\alpha)\ [-\ln(1-\alpha)]^{2/3}$	$[-\ln(1-\alpha)]^{1/3}$
	A_4	$4(1-\alpha)\ [-\ln(1-\alpha)]^{3/4}$	$[-\ln(1-\alpha)]^{1/4}$
Geometrical contraction model			
Contracting Area	R_2	$2(1-\alpha)^{1/2}$	$1-(1-\alpha)^{1/2}$
	R_3	$3(1-\alpha)^{2/3}$	$1-(1-\alpha)^{1/3}$
Diffusion method			
Diffusion	D_1	$(½)\alpha^{-1}$	α^2
	D_2	$[-\ln(1-\alpha)]^{-1}$	$(1-\alpha)\ln(1-\alpha)+\alpha$
	D_3	$(3/2)\ (1-\alpha)^{2/3}[1-(1-\alpha)^{1/3}]^{-1}$	$[1-(1-\alpha)^{1/3}]^2$
	D_4	$(3/2)\ [(1-\alpha)^{(-1/3)}-1]^{-1}$	$1-(2/3)\ \alpha-(1-\alpha)^{2/3}$
Reaction order model			
Reaction order	F_0	1	α
	F_1	$1-\alpha$	$[-\ln(1-\alpha)]$
	$F_{1.5}$	$(1-\alpha)^{3/2}$	$2[(1-\alpha)^{-1//2}-1]$
	F_2	$(1-\alpha)^2$	$[\alpha/(1-\alpha)]$
	$F_{2.5}$	$(1-\alpha)^{2.5}$	$(2/3)\ [(1-\alpha)^{-3/2}-1]$
	F_3	$(1-\alpha)^3$	$(1/2)\ [(1-\alpha)^{-2}-1]$
	F_4	$(1-\alpha)^4$	$(1/3)\ [(1-\alpha)^{-3}-1]$
	F_5	$(1-\alpha)^5$	$(1/4)\ [(1-\alpha)^{-4}-1]$

Table S2. Different type of linear iso conversional method

Iso-conversional model	Approximation p(x) value, Where, $x=\frac{Ea}{RT}$	Equation	Plot	Ea	A
KAS	$\frac{e^{-x}}{x^2}$	$\ln\left(\frac{\beta}{T^2}\right)=\ln\left(\frac{-AR\left(1-\frac{2RT}{Ea}\right)}{Ea\ln\alpha}\right)-\frac{Ea}{RT}$	$\ln\left(\frac{\beta}{T^2}\right)$ Vs $\frac{1}{T}$	Slope×(−R)	$\frac{(-(Ea)^2)}{(EaR\text{-}2R^2T)}\times e^{y\text{-}intercept}\times\ln\alpha$
FWO	$e^{(-2.315-0.4567x)}$	$\ln\beta=\frac{\ln AEa}{1-\alpha}-5.331-1.052\left(\frac{Ea}{RT}\right)$	$\ln\beta$ Vs $\frac{1}{T}$	$\text{Slope}\times\left(-\frac{R}{1.052}\right)$	$\left(\frac{R\times(1-\alpha)\times e^{y\text{-}intercept}}{Ea}\right)+5.331$
STR	$\frac{e^{-1.0008x}-0.312}{x^{1.92}}$	$\ln\left(\frac{\beta}{T^{1.92}}\right)=\ln\left(\frac{AEa}{1-\alpha}\right)-0.312-1.0008\left(\frac{Ea}{RT}\right)$	$\ln\left(\frac{\beta}{T^{1.92}}\right)$ Vs $\frac{1}{T}$	$\text{Slope}\times\left(-\frac{R}{1.0008}\right)$	$\left(\frac{(1-\alpha)\times e^{y\text{-}intercept}}{Ea}\right)$
FRM	No approximation	$\ln\left(\frac{d\alpha}{dt}\right)=\ln[A(1-\alpha)]-\frac{Ea}{RT}$	$\ln\left(\frac{d\alpha}{dt}\right)$ Vs $\frac{1}{T}$	Slope×(−R)	$\frac{e^{y\text{-}intercept}}{1-\alpha}$
LTA	No approximation	$\int_0^{\alpha}\ln\left(\frac{d\alpha}{dt}\right)_{\alpha,i}d\alpha=G(\alpha)-\frac{Ea}{R}\int_0^{\alpha}\left(\frac{1}{T}\right)_{\alpha,i}d\alpha$ where, $G(\alpha)=\alpha\ln A+\int_0^{\alpha}\ln[f(\alpha)]d\alpha$	$\int_0^{\alpha}\ln\left(\frac{d\alpha}{dt}\right)_{\alpha,i}$ Vs $\int_0^{\alpha}\left(\frac{1}{T}\right)_{\alpha,i}$	Slope×(−R)	$e^{\{y\text{-}intercept-(\alpha-1)\ln(1-\alpha)-\alpha\}}$

Table S3. Non-linear iso conversional method

Iso-conversional model	Approximation p(x)	Equation
VYZ	$\frac{e^{-x}}{x^2}\left(\frac{x^7+70x^6+1{,}886x^5+24{,}920x^4+170{,}136x^3+577{,}584x^2+844{,}560x+357{,}120}{x^8+72x^7+2{,}024x^6+28{,}560x^5+216{,}720x^4+880{,}320x^3+1{,}794{,}240x^2+1{,}572{,}480x+403{,}200}\right)$ (9)	$\Omega(E_\alpha)=\sum_{i=1}^{n}\sum_{j\neq i}^{n}\frac{I(E,T_{\alpha,i})\beta_j}{I(E,T_{\alpha,j})\beta_i}=\min$ (10)

Where, $p(x)=\frac{Ea}{RT}$, and $I(E,T_\alpha)=\int_0^{\alpha}e^{\left(\frac{-E_\alpha}{KT}\right)}dT=\left(\frac{E_\alpha}{R}\right)p(x)$ (11)

n=Number of experiments at different heating rates.

Here, $I(E,T_{\alpha,i})$ and $I(E,T_{\alpha,j})$ denote the integral temperature p(x) which deals with the heating rate programs β_i and β_j respectively. $I(E,T_\alpha)$ have no analytical solution. However, the value of $I(E,T_\alpha)$ can be calculated by direct numerical integration or by utilizing the Senum-Yang approximation.

At first, put the value of R and T at a particular α value for a particular heating rate in Eq. (9). Assuming a value of Ea and finding the value of p(x) for a particular α value and heating rate. Similarly, at the same value of Ea and α, find the p(x) value for another heating rate. With the help of different values of p(x) for the different heating rates at particular α values and Eqs. (10) and (11), minimizing the value of $\Omega(E_\alpha)$. Among the assuming Ea values, the assuming Ea value for which the value of $\Omega(E_\alpha)$ is minimum that assuming Ea value is considered as Ea for that α value and heating rate. In this way, the Ea value for a particular conversion is evaluated.

Table S4. Order of reaction calculated by AVM theory

Temperature (°C)	Slope	Order
150	−0.349	0.349
200	−0.233	0.233
250	−0.258	0.258
300	−0.212	0.212
350	−0.168	0.168
400	−0.016	0.016
450	−0.027	0.027

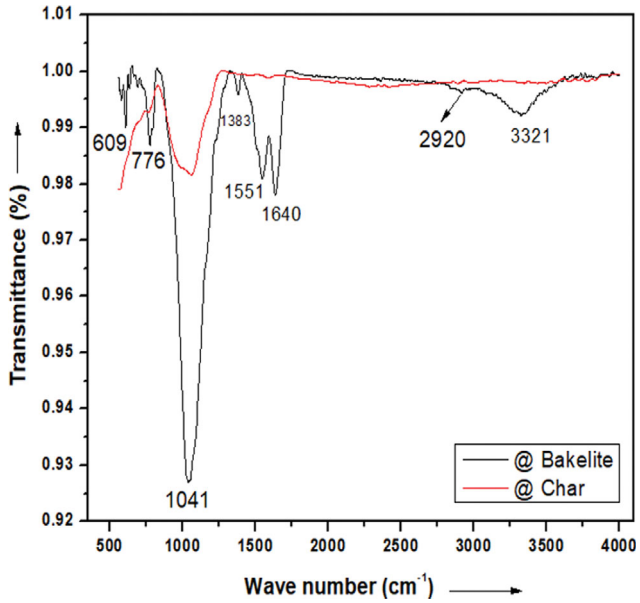

Fig. S1. FTIR analysis of discarded Bakelite and char produced from discarded Bakelite.

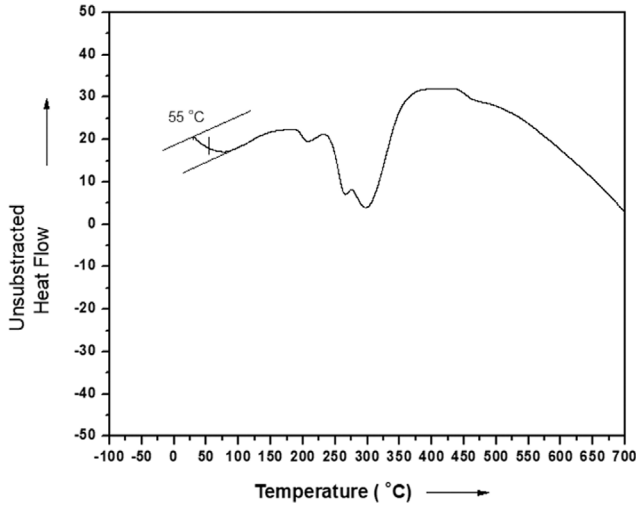

Fig. S2. DSC curve of discarded Bakelite at 30 °C/min.

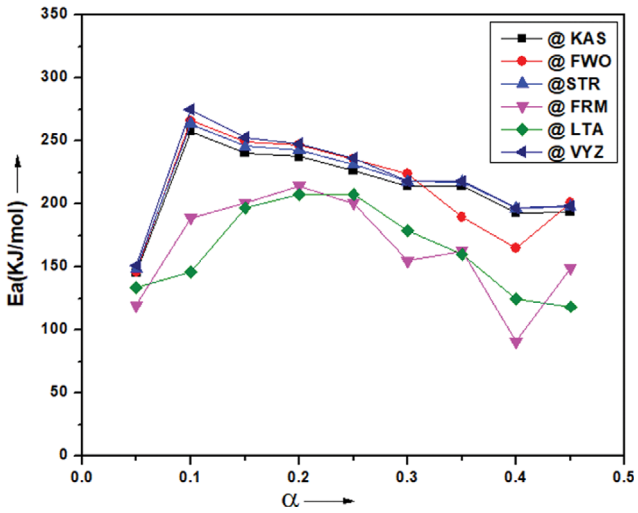

Fig. S3. Plot between mean Ea value and conversion.

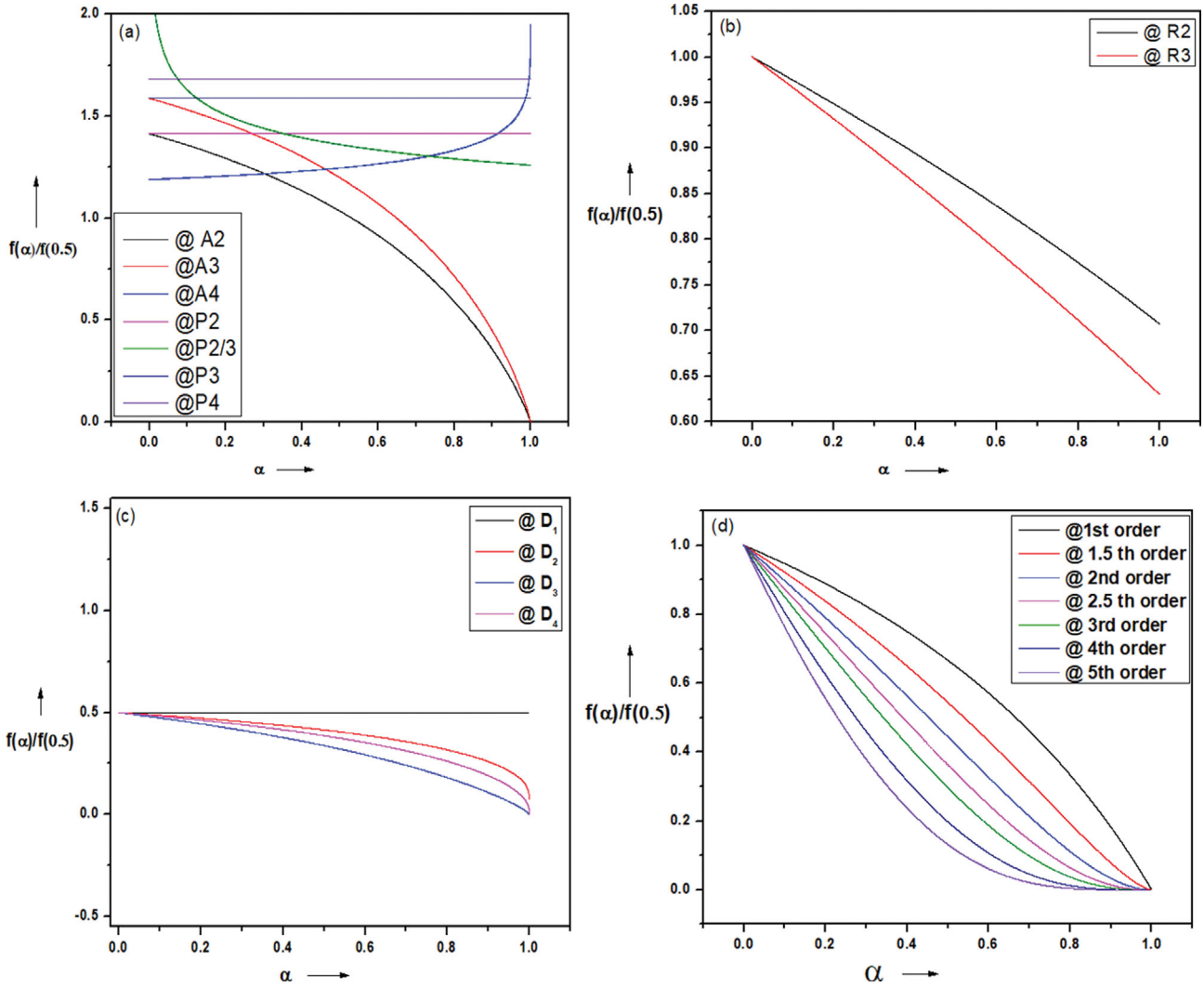

Fig. S4. Master plots showing (a) Nucleation model (b) Geometrical contraction model (c) Diffusion model (d) Reaction order model.

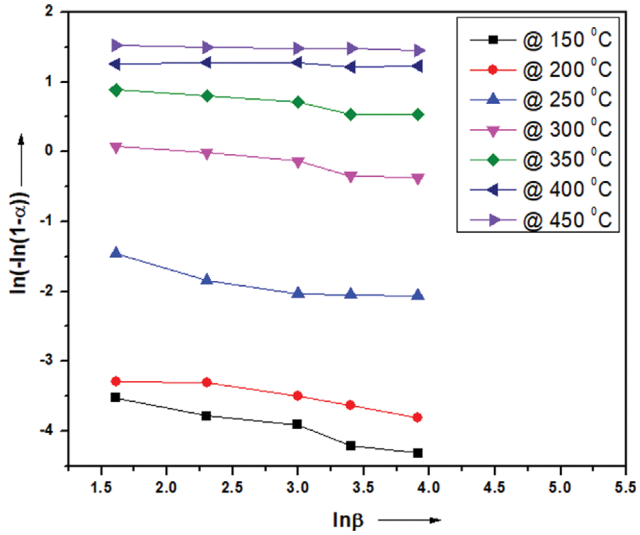

Fig. S5. Curves for order of reaction calculation by AVM theory.